Oscillating bacterial expression states generate herd immunity to viral infection

Christopher J. R. Turkington [a,c], Andrey Morozov [b], Martha R. J. Clokie[c], Christopher D. Bayliss[a]#

Department of Genetics and Genome Biology, University of Leicester, Leicester, United Kingdom[a]; Department of Mathematics, University of Leicester, Leicester, United Kingdom[b]; Department of Infection, Immunity, and Inflammation, Leicester, United Kingdom[c]

Running Head: Bacterial herd immunity against viral infection

#Address correspondence to Christopher D. Bayliss, cdb12@le.ac.uk

Abstract word count = 184

Main text word count = 4527

Abstract:

Hypermutable loci are widespread in bacteria as mechanisms for rapid generation of phenotypic diversity, enabling individual populations to survive fluctuating, often antagonistic, selection pressures. As observed for adaptive immunity, hypermutation may facilitate survival of multiple, spatially-separated bacterial populations. We developed an 'oscillating prey assay' to examine bacteriophage (phage) spread through populations of *Haemophilus influenzae* whose phage receptor gene, *lic2A*, is switched 'ON' and 'OFF' by mutations in a hypermutable tetranucleotide repeat tract. Phage extinction was frequently observed when the proportion of phage-resistant sub-populations exceeded 34%. *In silico* modelling indicated that phage extinction was interdependent on phage loss during transfer between populations and the frequency of resistant populations. In a fixed-area oscillating prey assay, heterogeneity in phage resistance was observed to generate vast differences in phage densities across multiple bacterial populations resulting in protective quarantining of some populations from phage attack. We conclude that phase-variable hypermutable loci produce bacterial 'herd immunity' with resistant intermediary-populations acting as a barricade to reduce the viral load faced by phage-sensitive sub-populations. This paradigm of meta-population protection is applicable to evolution of hypermutable loci in multiple bacteria-phage and host-pathogen interactions.

Importance

Herd immunity is a survival strategy wherein populations are protected against invading pathogens by resistant individuals within the population acting as a barrier to spread of the infectious agent. Although, this concept is normally only applied to higher

47 eukaryotes, prokaryotic organisms also face invasion by infectious agents, such as
48 bacterial viruses, bacteriophage (phage). Here we use novel experimental approaches and
49 mathematical modelling, to show that bacteria exhibit a form of herd immunity through
50 stochastically generated resistant variants acting as barricades to phage predation of
51 sensitive cells. With hypermutable loci found in many prokaryotic systems, this
52 phenomenon may be widely applicable to phage-bacteria interactions and could even
53 impact phage-driven evolution in bacteria.
54
55 **Introduction**

56 Hypermutable loci as mediators of survival against constantly fluctuating
57 selection pressures are a predictable outcome of the evolution of evolvability as stated in
58 the Red Queen hypothesis (1, 2). Fluctuating selection pressures are regularly faced by
59 bacteria during persistence in human hosts, where bacteria adhere to host surfaces while
60 contending with varying nutrient concentrations, frequent exposure to immune effectors
61 and predation by bacteriophages. These fluctuations often select for and against opposing
62 gene expression states of single loci leading to evolution of localised hypermutable
63 mechanisms that produce frequent switches in single-gene expression states.

64 One class of hypermutable loci facilitate survival of conflicting selective
65 pressures by pre-emptive, frequent, and reversible 'ON/OFF' generation of adaptive
66 variants, in a process known as 'phase variation' (PV; 2–5). A major mechanism of PV
67 involves increases and decreases in identical, tandemly-arranged DNA repeats
68 (microsatellites) by slipped strand mispairing during DNA replication (3, 5, 6). The
69 obligate human respiratory commensal and pathogen *H. influenzae* contains an expansive

array of repeat driven phase variable loci (7–13). Several of these loci are required for addition of sugar molecules onto the surface-exposed outer-core of the lipooligosaccharide (LOS) (5, 7). PV of the UDP-galactose-LOS-galactosyltransferase encoding gene, *lic2A*, is mediated by a 5'CAAT repetitive tract present in the open-reading frame (14). Phage HP1c1 attaches to an LOS epitope of *H. influenzae* strain Rd that contains the galactose sugar added by *lic2A* (15). PV of *lic2A* causes switching between phage sensitive (*lic2A* ON) and phage resistant states (*lic2A* OFF) (15, 16). Partial resistance to phage HP1c1 in strain Rd is also mediated by PV of a Type I restriction-modification (RM) system. PV of surface receptors and RM systems generates resistance to phage infection in several bacterial species (17–22).

While phage-receptor PV prevents viral propagation in individual populations, the frequency and distribution of resistant variants within larger meta-populations may also impose inhibitory effects on phage spread through multiple spatially-linked sub-populations. In order to explore this potential benefit, we examined how diversity in phage resistance/sensitivity phenotypes generated by one hypermutable locus, *lic2A*, alters spread of phage HP1c1.

RESULTS

Low numbers of resistant bacterial populations significantly restrict phage spread and densities. PV can generate high levels of ON and OFF variants of single genes within individual populations but also has the potential to generate population-to-population variation within a meta-population. For example, *lic2A*-positive *H. influenzae* colonies on agar plates will have most cells in a *lic2A* ON expression state but will also

93 contain small, but significant, numbers of *lic2A* OFF variants. Similarly, an *H. influenzae*
94 meta-population may consist of multiple sub-populations with one fraction being *lic2A*-
95 positive and another fraction being *lic2A*-negative. Such population-to-population
96 variation is observed for *H. influenzae* colonies on agar plates and for *H. influenzae*
97 populations isolated from artificially-inoculated animals and asymptomatic human
98 carriers (23–27). Proportions of ON and OFF sub-populations in a meta-population will
99 depend on levels of selection for each expression state and on 'founder' effects that
100 influence the starting state of each sub-population. Thus, any phage invading a bacterial
101 meta-population where there is PV of the receptor must contend with highly variable
102 distributions of resistance and sensitive sub-populations.

103 To simulate the effect of phage-receptor PV on spread of phage through bacterial
104 meta-populations we developed the 'oscillating prey assay' (Fig. 1). This assay involves
105 continual cycling of phage through *H. influenzae* strain Rd cultures with either a majority
106 *lic2A* ON or OFF phenotype. Each cycle allows for one round of phage replication after
107 which the phage-containing supernatant is recovered, filtered, and transferred to a new
108 culture of either *lic2A* ON or OFF *H. influenzae* cells. During transfer, the supernatant is
109 subject to a 10-fold dilution. This arbitrary dilution factor simulates loss of phage during
110 population-to-population transmission.

111 Six population structures were examined in the oscillating prey assay: [1] 100 %
112 ON (HP1c1 cycled only through *lic2A* ON populations; S100), [2] 66 % ON (2:1 *lic2A*
113 ON:OFF; S66), [3] 50 % ON (1:1 *lic2A* ON:OFF, starting with an ON culture; S50), [4]
114 50 % OFF (1:1 *lic2A* ON:OFF, starting with an OFF culture; R50), [5] 66 % OFF (1:2
115 *lic2A* ON:OFF; R66), and [6] 100 % OFF (HP1c1 cycled only through *lic2A* OFF

116 populations; R100). Survival and propagation of phage was dependent on the proportion
117 of phage-resistant sub-populations in each series of 20 cycles (Fig. 2). Survival of phage
118 to the final cycle was only observed when the proportion of phage-resistance populations
119 was ≤ 34% (i.e. the S66 and S100 populations; Fig. 2). Extinction events occurred within
120 5 to 16 cycles in all other heterogeneous and homogeneous populations at a rate that was
121 dependent on the proportion of resistant sub-populations. Despite survival of phage
122 through to cycle 20 in the S66 population series, phage densities were significantly
123 decreased by this cycling regime (Fig. 2; paired *t*-test: $t = 4.97$, $P < 0.05$; mean ± SEM
124 PFU/mL values for phage densities at cycle 0 = $7.16 \pm 0.26 \times 10^5$ and cycle 20 =
125 $2.82 \pm 0.9 \times 10^4$), indicating that further passages with a similar pattern would have
126 resulted in phage extinction. Contrastingly, phage density increased when all sub-
127 populations were phage sensitive (S100), with phage densities plateauing after ~11
128 cycles. Thus, both phage survival and density were limited by the frequency of
129 encounters with phage-resistant *lic2A* OFF phase variants during passage through a linear
130 series of sub-populations.

131 **Detection of combinatorial effects of population structure and dilution rate**
132 **on phage extinction using an *in-silico* model of phage spread**. Our experimental data
133 indicated that meta-population structure had a major impact on phage survival and
134 spread. In order to explore a wider range of linear and non-linear cycling patterns and the
135 effects of dilution rate, we developed a mathematical model of the oscillating prey assay.
136 This model utilized key phage parameters for adsorption rate, replication time, burst size
137 and stability of phage HP1c1 (see Fig. S1). The number of oscillations was extended to
138 105 phage replicative cycles, while cycling patterns were randomised for each specific

overall proportion of *lic2A* ON/OFF sub-populations. The mathematical model produced comparable findings to the experimental setting (Fig. S2). Multiple runs of this model exhibited stochastic variation in phage densities and extinction events as observed in the experimental model but with extinction events occurring over a wider band of replication cycles (Fig. 3A-B). This model demonstrates that random patterns of ON/OFF expression states for a phage receptor can limit phage spread.

Multiple simulations (n = 200) were performed for each combination of R (the percentage of phage-resistant *lic2A* OFF sub-populations) and C (the inverse of the dilution coefficient). Average phage densities were measured for all cycles and runs of each combination of R and C, and phage extinction was defined to occur whenever the density fell below 100 PFU/mL. Phage extinction was always observed when the number of resistant states exceeded 70% of sub-populations, even at a low dilution rate of 1 in 2 (C=0.5; Fig. 3C). Similarly, when phage loss was ≥ 98 % at each transfer (i.e. C=0.02), phage extinction was observed for all meta-population structures except those consisting of >95% phage-sensitive sub-populations (Fig. 3C). Between these extremes, there was an accelerating trade-off between R and C with respect to phage extinction and average phage density; decreases in dilution rate were countered by a high prevalence of resistant sub-populations enabling bacterial populations to survive even when phage dispersal was low (Fig. 3C). This observation suggests that on-going evolution of localised hypermutability for a surface-exposed bacterial epitope could be tuned to the prevalence and density of phages capable of using the phase-variable epitope as a receptor for surface attachment.

Localised hypermutation-driven herd-immunity produces regional variations in phage densities within bacterial meta-populations. Both our experimental and *in silico* oscillating prey assays demonstrated that phage spread was influenced by the linear pattern of phase-variant sub-populations. However, the distribution of phase variants across a surface (e.g. microcolonies on upper respiratory tract surfaces for *H. influenzae*) is anticipated to be random and hence to result in spatial effects on phage spread. Indeed, spatially structured environments are known to restrict phage spread (28). Spatial structuring was explored by examining phage transmission across meta-populations of fixed dimensions but with varying proportions of each *lic2A* expression state (Fig. S3). This fixed-area oscillating prey assay was initiated by inoculating phage into one well of a 96-well plate and then expanding outward by seeding each subsequent replicative cycle into neighbouring wells (see Fig. S4).

Passage of HP1c1 through heterogeneous populations of the fixed-area oscillating prey assay resulted in uneven phage densities across the meta-populations consisting of 50-66% phage-sensitive populations (Fig. 4B-4D). Conversely, homogenous densities were observed for high (Fig. 4A) or low (Fig. 4E and 4F) phage-sensitive distributions. When 66% of populations were phage-sensitive (Fig. 4B), densities ranged from 10^3 to 10^{10} PFU/mL, whereas densities always exceeded 10^8 PFU/mL if all population were sensitive (Fig. 4A). Phage densities in specific regions of heterogeneous populations were dependent on the direction of propagation with passage through multiple resistant or sensitive sub-populations resulting in low or high phage densities, respectively. This model shows how spatial meta-population heterogeneity could prevent equal dissemination of phage through host populations with phase-variable phage-receptors and

aid survival of phage-sensitive sub-populations whose phenotypes may be beneficial for bacterial survival against other selective pressures.

Observed PV rates generate populations with phase-variant proportions capable of herd-immunity. The fixed-area oscillating prey assay outputs showed how phage extinction was dependent on the proportion of phage-resistant sub-populations. *H. influenzae* normally resides in the upper respiratory tract where selection is likely to act on both PV states of a locus. Thus, the proportion of resistant populations depends on both selection strength for/against the phage-resistance phenotype, and the ON/OFF switching rate. Switching rates of *H. influenzae* phase-variable genes are malleable due to changes in repeat number and can evolve in response to alternating selection pressures (28, 29).

A mathematical model was developed to examine the impact of different switching rates and immune selection on the proportions of *lic2A* expression states (Fig. 5 and Supplementary Data S1). Dixon *et al.* (30) found that the *lic2A* ON-to-OFF (S-to-R; where R and S are the phage-resistant and phage-sensitive states, respectively) switching rate was 1.7-fold higher than the *lic2A* OFF-to-ON (R-to-S) switching rate. The mathematical model assumed that these proportions were maintained for three 10-fold differences in overall mutation rate representing low, intermediate and high repeats numbers (Fig. 5A-5C). In the absence of any selective difference between the S and R states (m=1), a high, steady-state proportion (>63%) of R, was observed for all mutation rates but with minor differences in the rate of approach to the steady state and absolute amounts of R. The *lic2A* OFF state (i.e. R) is known to be more immune sensitive than the ON state (i.e. S), we therefore imposed a selection against R. Even with strong

207 selection (m=0.99), high levels of R were maintained by medium to high switching rates
208 (Fig. 5A and 5C, respectively). In contrast, when switching rates were low (Fig. 5B),
209 even weak selection (m=0.999) drives resistant variants to <1% (Fig. 5B). Our other *in*
210 *silico* models indicated that phage spread was inhibited when the probability of
211 encountering R variants was between 10-70% for dilution rates of 0.02 to 0.6. Thus, the
212 immune model shows that observed repeat numbers and switching rates for the *lic2A*
213 gene of *H. influenzae* strains can maintain sufficient phage-resistant variants for
214 restricting phage spread even when there is immune selection against this state.

215

216 **DISCUSSION**

217 Hypermutable loci have well-documented roles in facilitating survival of
218 individual bacterial populations against phage predation through generation of phage-
219 resistant cells. An unexplored concept is that hypermutation driven heterogeneity in
220 phage resistance across the wider population also facilitates bacterial survival of phage
221 predation.

222 **Phase-variable loci can generate herd immunity in bacterial meta-**
223 **populations**. The concept of herd immunity was derived to explain the protection of
224 susceptible individuals in populations with high levels of immunity to an infectious agent
225 as observed for measles in Baltimore (31). Ordinarily applied to naturally or vaccine-
226 acquired immunity to infectious agents in human populations (32), we show, herein, that
227 repeat-mediated PV of a phage-receptor provides a form of 'bacterial herd-immunity' at
228 the population level (Fig. 6). Thus, phage spread is retarded by resistant sub-populations
229 creating barriers between the phage and phage-sensitive bacterial sub-populations as

shown in our one- and multidirectional experimental models (Fig. 2 and Fig. 5), and an *in silico* model with randomized patterns of phage sensitivity (Fig. 3). Key features of these models were that: the chance of phage survival was inversely proportional to the linear pattern of resistance faced by the phage population; random distributions of phage-resistant/sensitive populations result in large variations in viral numbers across a meta-population with some regions being completely free of phage; and dilution during transfer of phage between populations modulates the number of phage-resistant populations required to retard phage spread. Thus, localised hypermutation of a phage-receptor generates herd-immunity whereby phage-sensitive sub-populations can be maintained at high levels within bacterial meta-populations.

PV of phage receptors or RM systems is an established phenomenon observed across numerous species and occurring by multiple mechanism. Repeat-mediated switching due to hypermutation of polyG tracts in phage receptor genes of *C. jejuni* strain NCTC11168 abrogates infection by phage F336 (19). Similar polyG hypermutation controls the phage growth limitation system of *Streptomyces coelicor* A3(2) and confers resistance to infection with phage φC31 (33). Epigenetic PV of Ag43 in *E. coli* or the gtr^{P22} operons that control O-antigen modification in *Salmonella* are known or proposed to modulate phage infection (34, 35). High frequency, but not hypermutable, mutations in short polyG or polyA tracts produce resistance to phages in both *Bordetella pertussis* (36) and *Vibrio cholerae* (17). Although these mechanisms vary in the rates of generation of phage resistant variants and in the strength of phage resistance (e.g. high for receptor PV and low for RM PV), they all have the potential to generate spatially-structured populations and hence herd immunity to phage infection.

253 Additionally, there is potential for evolution of the herd immunity state. PV rates
254 can evolve through changes in the mutable mechanism. Thus repeat-mediated PV rates
255 increase as a function of tract length. We anticipate that frequent exposure to phage
256 would select for a greater capacity to form heterogeneous meta-populations through
257 secondary selection for an increase in mutability of the phage receptor.

258 **Evidence for immune-driven selection of lic2A ON expression states.** One
259 rationale for the existence of PV-driven herd immunity is that protection of the phage-
260 sensitive state is required because this state is advantageous under certain circumstances.
261 For *lic2A*, the ON state in *H. influenzae* strain Rd is phage-sensitive and this states leads
262 to extension of the LOS side-chain from the third heptose with a single galactose, a
263 digalactose or more complex sugars. In *in vitro* studies, *lic2A*-dependent epitopes aid in
264 survival against human immune responses (16), with the LOS extensions associated with
265 *lic2A* expression encoding epitopes also present on the human P blood group antigens
266 (37). Although human volunteer studies of colonisation with *H. influenzae* have found
267 that expression of *lic2A* was not essential for human nasopharyngeal colonisation (26),
268 the *lic2A* ON state has been associated with disease states, including non-typeable *H.*
269 *influenzae* pneumonia (24). We performed an analysis of 104 *H. influenzae* genome
270 sequences and found that *lic2A* is in an ON state in ~63% of all isolates and is
271 predominantly in the ON state for multiple disease conditions, suggesting selection for
272 expression of *lic2A* occurs across a wide range of niches for *H. influenzae* (Fig. S5).
273 These observations are consistent with a scenario where phage drive evolution of
274 hypermutability rates as the *lic2A* gene oscillates between selection for/against the
275 immune-resistant/phage-sensitive and immune-sensitive/phage-resistant states. A caveat

276 to these conclusions is phage-specificity as phage HP1c1 may be specific to extension of
277 the third heptose of *H. influenzae* LOS whereas Lic2A can, in the appropriate genetic
278 context, generate extensions from any of the three heptoses of the LOS inner core.
279 Further work is required to determine whether HP1c1 is specific for extension from the
280 third heptose and if other phages can target this epitope in *H. influenzae* strains where
281 extension is from the first or second heptose.

282 **Transmission and the 'phage loss' phenomenon.** Our mathematical model of
283 herd immunity indicates that phage spread is interdependent on population structure and
284 the rate of phage loss from the environment by dilution. Thus, when dilution rates are
285 high, phage extinction events are frequent despite high levels of sensitivity within the
286 bacterial population. While natural rates of phage loss from respiratory environments is
287 unknown, a number of factors have the capacity to impact phage loss, such as humidity,
288 salinity and immune responses (38–41). For phage infections of human commensals or
289 pathogens, such as *H. influenzae*, more extreme environmental selection pressures will
290 apply as phages are transmitted between carriers of target bacterial species.

291 There are two potential extreme scenarios where the herd immunity model is
292 applicable and 'phage loss' is either low or high. These scenarios are elaborated for *H.*
293 *influenzae* but are relevant to other bacterial commensals/pathogenic bacteria. Firstly,
294 colonisation of asymptomatic carriers by *H. influenzae* is likely to involve a series of
295 microcolonies, a meta-population, distributed across the nasopharyngeal surface rather
296 than one continuous population. Phage will therefore have to transmit between
297 microcolonies thereby imposing a low potential for phage loss such that only high
298 numbers of phage-resistant populations will provide protection for any phage-sensitive

299 microcolonies. A second scenario is a population of *H. influenzae* carriers, in this case
300 phage transmission between carriers is likely to result in significant phage loss and hence
301 low numbers of carriers colonized by phage-resistant populations could prevent phage
302 spread to all carriers. These scenarios illustrate the central role of transmission in shaping
303 bacterial herd immunity and in the impact of this fitness trait on localised hypermutation
304 of the phage receptor.

305 **Bacterial herd immunity could impact on phage-driven evolution.** We
306 observed that phage densities were highly variable across spatially-structured bacterial
307 populations with some regions exhibiting a complete absence of phage (Fig. 6). This
308 imposition of spatially-discrete levels of phage selection could select for alternative
309 adaptive traits within the bacterial host. In studies of *Caulobacter crescentus*, low phage
310 selection led to isolation of >200 phage resistance mechanisms, while only ~60 distinct
311 resistance forms were isolated during high phage selection (42). Thus, bacterial herd-
312 immunity may prevent uniformity in phage selection pressures across bacterial meta-
313 populations leading to evolution of distinct phage-resistance mechanisms within a single
314 clonal lineage.

315 In summary, our demonstration of a hypermutable locus retarding spread of an
316 infectious agent within a prokaryotic meta-population suggests that the herd immunity
317 phenomenon may be applicable to a wide variety of interacting biological organisms and
318 have deep evolutionary roots. Our conceptual framework could be utilised to explore
319 whether somatic hypermutation, a key example of localised hypermutation in eukaryotes,
320 evolved through selection for sub-population heterogeneity linked to pathogen resistance.

321

MATERIALS AND METHODS

Phage and bacterial strains used in this study. Phage HP1c1, and the *lic2A* ON (Rd 30S) and OFF (Rd 30R) phase variants of *H. influenzae* were obtained from A. Piekarowicz (University of Warsaw, Poland). Phage HP1c1 is maintained in the lysogenic state within *H. influenzae* RM118-L. *H. influenzae* strains were cultured overnight at 37ºC on 1% BHI agar supplemented with 10% Leventhal's supplement and 2 µg/mL nicotinamide adenine dinucleotide (NAD) or in 10 mL BHI broth supplemented with 2 µg/mL NAD and 10 µg/mL hemin (sBHI).

Phage HP1c1 stocks. Mitomycin C was added to a concentration of 300 ng/mL to an OD_{600} 0.1 culture of RM118-L in 10 ml of sBHI. After incubation for 8 hours, the culture was centrifuged (4,946x*g*, 4ºC, 10 minutes) and then the supernatant was passed through a 0.22 µm syringe filter to obtain a phage suspension, which was stored at 4ºC.

High titer phage stocks were propagated in *H. influenzae* Rd 30S by adding 100 µL of induced phage to mid-log phase cultures diluted to an OD_{600} of 0.01 in 10 ml sBHI and incubating for 8 hours. Cultures were processed as described above.

Determination of phage titers. Phage titers were determined using the small-drop plating assay (43). Briefly, 150 µl of a mid-log phase Rd 30S culture, OD_{600} 0.1, was added to 3 mL of 0.3 % BHI agar (supplemented with 2 µg/mL NAD and 10 µg/mL hemin), mixed by inversion, and poured onto 1% BHI agar plates supplemented with 10% Leventhal's media and 2 µg/mL NAD. Ten-fold serial dilutions were spotted in triplicate 10 µl drops onto the soft agar (the minimum detection threshold is 33.3 PFU/mL).

Oscillating prey assay. Two phase variants, namely, Rd 30S (*lic2A* ON, phage sensitive variant) and Rd 30R (*lic2A* OFF, phage resistant variant) were utilized to generate the following three-repeat host population-cycling patterns: S100, ON-ON-ON; S66, ON-ON-OFF; S50, ON-OFF-ON; R50, OFF-ON-OFF; R66, OFF-OFF-ON; R100, OFF-OFF-OFF. *H. influenzae* Rd 30S and Rd 30R were sub-cultured as described above in 20 mL of sBHI to an OD_{600} of 0.1. A 5 mL aliquot of the relevant strain was inoculated with HP1c1 at MOI ~0.01. Cultures were adjusted to 6 mL, mixed by inversion and 1 mL was removed for filtration and determination of the T = 0 phage titre. The remaining 5 mL was incubated for 50 minutes (i.e. one viral replication cycle) at 37ºC with shaking and then filtered for phage quantification. Subsequent cycles were initiated by transferring 600 µl of filtrate to a fresh 5 mL culture of relevant *lic2A* phase variant. Five phage transfers were conducted per day with phage-containing filtrates being stored overnight at 4ºC.

Fixed-area oscillating prey assay. Six cycling frequencies were tested (Fig. 5). Allocation of each phase variant (i.e. Rd 30S or Rd 30R) to specific wells was determined by numbering wells from 1 to 631 followed by randomization of these numbers into two sets using R (see Fig. S3). One phase variant was added to the first set of numbered wells and the other phase variant to the second set.

Rd 30S and Rd 30R were sub-cultured to OD_{600} 0.1 and then 250 µL of appropriate culture was added to the starter well. Phage HP1c1 was added at a final concentration of ~1 x 10^6 PFU/mL to this well and the volume was adjusted to 300 µL with fresh sBHI broth. After mixing by tituration, 100 µL was removed for phage titration. The plate was incubated at 37ºC with shaking for 70 minutes (a longer incubation time was required in

this miniaturised oscillating prey assay for completion of one phage replication cycle [data not shown]). Following incubation, the plate was centrifuged at 1500 x *g* for 4 minutes to pellet bacterial cells and then 20 µl of supernatant was transferred to surrounding wells (see Fig. S4). Remaining supernatant was harvested for phage titration. Newly-inoculated wells received 167 µl of a fresh OD_{600} 0.1 culture of either Rd 30S or Rd 30R, depending on the cycling pattern, followed by repetition of all previously described steps. Ten cycles were performed in the left, right, and downward directions, and 20 cycles in the upward direction (see Fig. S3 and S4). Five transfers and cycles were conducted each day with the 96-well plates being wrapped in paraffin film and stored at 4°C overnight. This assay was conducted once for each population structure.

Survey of Lic2A expression state in multiple *H. influenzae* genomes. A set of 126 genomes available in GenBank as of 06-09-2016 were screened with blast2seq for the presence of genes homologous to the *lic2A* gene of *H. influenzae* strain Rd KW20. *Lic2A* homologues were found in 121 of the 126 genomes but only 104 could be analysed due to incomplete sequence coverage in 17 genomes. The ON state was identified by the presence of a full length amino acid product (~300 amino acids). The 5'CAAT repeat numbers were determined by visual inspection of aligned sequences. All metadata, where available, was collated from the GenBank entry for each genome, or references associated with each strain.

Mathematical model and simulations. We describe bacteria-phage interaction using the conventional modelling approach (45, 46). Dynamics of bacteria and phage densities in each experimental cycle (transfer) of number n within time T_0=40min (i.e. before the start of mass replication of phages) is given by

390 $$\frac{dB_0}{dt} = -KPB_0 ,$$

391 $$\frac{dB_i}{dt} = KPB_{i-1} - KPB_i, \quad i = 1,..., N-1$$

392 $$\frac{dB_N}{dt} = KPB_{N-1} ,$$

393 $$\frac{dP}{dt} = -PK\sum_{i=0}^{N-1} B_i - mP \quad , nT < t < T\,n + T_0,$$

394 where B_0 is the number/density of phage-free bacteria; B_i is the number/density of
395 bacteria with i phage attachments; P is the number/density of free phages. The maximal
396 number of phage attachments for an individual bacterial cell is given by N. In the model,
397 we assume that the injection rate is very fast (i.e. instantaneous), so that attachment of
398 one phage immediately results in an infection.

399 For simplicity, we assume that there is no bacterial growth. We also assume that all
400 phage attachments occurring within the first 10 minutes lead to replication (each phage
401 produces b new phages) whereas later attachments result in phage loss without
402 replication. We neglect binding of newly replicated phages within the last Δ= 10 min of
403 each cycle. The other model parameters are: K-, phage adsorption constant (note that this
404 constant is assumed to be independent from the number of bound phages and that K=0 for
405 phage-resistant bacteria); m, natural mortality of phages; b, phage burst size.

406 At the start of each experimental cycle (i.e. just after dilution) all bacteria are phage-
407 free and their number is always equal to B_S, in other words,

408 $$B_0\left(t = (Tn)^+\right) = B_s, \quad B_i\left(t = (Tn)^+\right) = 0 \quad , B_i(t = (Tn)^+) = 0 \quad , i=1,\ldots, N,$$

409 Here the symbol '+' denotes the time just after the n^{th} dilution, i.e. just prior to the
410 cycle (n+1); the symbol '−' denotes the time prior to the n^{th} dilution, i.e. at the very end
411 of cycle n.

412 The phage density is obtained from the final density in each cycle multiplied by the
413 dilution coefficient C_n in cycle #n (this value can vary between experiments).

414 $$P(t = (Tn)^{+}) = P(t = (Tn)^{-})C_n .$$

415 The density of phages just prior to dilution n (i.e. at the end of cycle #n) is
416 determined by

417 $$P(t = (Tn)^{-}) = \sum_{i=1}^{N} B_i(Tn - T_0)b + P_S(t = (Tn)^{-}) ,$$

418 where P_S are non-attached phages that survived to the end of the cycle; i.e. the phage
419 number at the cycle end, prior to dilution, is given by the number of infected bacteria at
420 time $T-T_0$ multiplied by the burst size b plus the number of surviving phages P_s.

421 Susceptible bacteria are characterized by K>0, whereas for resistant bacteria we
422 have K=0. The value of K is kept constant across each cycle of 50 minutes.

423 Model parameters and verification were derived from experimental settings or
424 findings. Direct observations indicated that B_S=1.75±0.25*10^8 cell/ml, T=50 min, and
425 T_0=40 min. The adsorption constant of K=7±3*10^{-10} mL/(cell min) was estimated from
426 an adsorption assay (Fig. S1). Other parameters were estimated directly from the
427 oscillating prey assay by model fitting (see Fig. S2): b=42±5 (burst size); and
428 m=0.006±0.003 1/min. The parameter N had a minor effect in our computation and hence
429 we utilised N =20 in all subsequent models.

Further simulations (e.g. Fig. 3c) considered the phage-bacterial dynamics across 105 cycles. Variations in the dilution rate C were simulated by changing the value of C according to $C=C*(1+\varepsilon)$, where ε is a normally distributed random variable with a mean of 0. and variance of 0.3^2 . In each cycle, K was randomly switched from $K= 7*10^{-10}$ (susceptible bacteria) to $K=0$ (resistant bacteria). The frequency of switching was determined by the probability p, which gives the probability of encountering susceptible bacteria. Examples simulations, shown in Fig. 3a and 3b, were constructed for $C=0.1$, $p=0.75$ (A) $p=0.85$ (B). Fig. 3c was obtained by repeating simulations across 105 for variable parameters C and p. Numerical simulation was based on the standard Runge-Kutta integration method of order 4 using MATLAB software. When phage density dropped to or below the low value threshold of $P_0=100$, we considered that this was equivalent to $P=0$ and stopped further simulations. The initial density of phages at time $t=0$ was $4.28*10^7$ PFU/mL.

FUNDING INFORMATION

C.J.R.T. was supported by the Biotechnology and Biological Sciences Research Council (BBSRC) [BB/J014532/1] and the College of Life Sciences of the University of Leicester.

REFERENCES

1. van Valen L. 1973. A new evolutionary law. Evol Theory 1:1–30.
2. Moxon ER, Rainey PB, Nowak MA, Lenski RE. 1994. Adaptive evolution of highly mutable loci in pathogenic bacteria. Curr Biol 4:24–33.

453 3. Bayliss CD. 2009. Determinants of phase variation rate and the fitness
454 implications of differing rates for bacterial pathogens and commensals. FEMS
455 Microbiol Rev 33:504–20.
456 4. Rainey PB, Beaumont HJE, Ferguson GC, Gallie J, Kost C, Libby E, Zhang X-X.
457 2011. The evolutionary emergence of stochastic phenotype switching in bacteria.
458 Microb Cell Fact 10 Suppl 1:S14.
459 5. Moxon ER, Bayliss CD, Hood DW. 2006. Bacterial contingency loci: the role of
460 simple sequence DNA repeats in bacterial adaptation. Annu Rev Genet 40:307–33.
461 6. van der Woude MW, Bäumler AJ. 2004. Phase and antigenic variation in bacteria.
462 Clin Microbiol Rev 17:581–611, table of contents.
463 7. Power PM, Sweetman W a, Gallacher NJ, Woodhall MR, Kumar G a, Moxon ER,
464 Hood DW. 2009. Simple sequence repeats in *Haemophilus influenzae*. Infect
465 Genet Evol 9:216–28.
466 8. Bayliss CD, Field D, Moxon ER. 2001. The simple sequence contingency loci of
467 *Haemophilus influenzae* and *Neisseria meningitidis*. J Clin Invest 107:657–62.
468 9. Kroll JS, Moxon ER. 1988. Capsulation and gene copy number at the cap locus of
469 *Haemophilus influenzae* type b. J Bacteriol 170:859–64.
470 10. Ren Z, Jin H, Whitby PW, Morton DJ, Stull TL. 1999. Role of CCAA nucleotide
471 repeats in regulation of hemoglobin and hemoglobin-haptoglobin binding protein
472 genes of *Haemophilus influenzae*. J Bacteriol 181:5865–70.
473 11. Dawid S, Barenkamp SJ, St Geme JW. 1999. Variation in expression of the
474 *Haemophilus influenzae* HMW adhesins: a prokaryotic system reminiscent of
475 eukaryotes. Proc Natl Acad Sci U S A 96:1077–82.

12. Glover SW, Piekarowicz A. 1972. Host specificity of DNA in *Haemophilus influenzae*: restriction and modification in strain Rd. Biochem Biophys Res Commun 46:1610–7.

13. De Bolle X, Bayliss CD, Field D, Van De Ven T, Saunders NJ, Hood DW, Moxon ER. 2000. The length of a tetranucleotide repeat tract in *Haemophilus influenzae* determines the phase variation rate of a gene with homology to type III DNA methyltransferases. Mol Microbiol 35:211–222.

14. High NJ, Deadman ME, Moxon ER. 1993. The role of a repetitive DNA motif (5'-CAAT-3') in the variable expression of the *Haemophilus influenzae* lipopolysaccharide epitope alpha Gal(1-4)beta Gal. Mol Microbiol 9:1275–82.

15. Zaleski P, Wojciechowski M, Piekarowicz A. 2005. The role of Dam methylation in phase variation of *Haemophilus influenzae* genes involved in defence against phage infection. Microbiology 151:3361–9.

16. Clark SE, Eichelberger KR, Weiser JN. 2013. Evasion of killing by human antibody and complement through multiple variations in the surface oligosaccharide of *Haemophilus influenzae*. Mol Microbiol 88:603–18.

17. Seed KD, Faruque SM, Mekalanos JJ, Calderwood SB, Qadri F, Camilli A. 2012. Phase variable O antigen biosynthetic genes control expression of the major protective antigen and bacteriophage receptor in *Vibrio cholerae* O1. PLoS Pathog 8:e1002917.

18. Cota I, Blanc-Potard AB, Casadesús J. 2012. STM2209-STM2208 (opvAB): a phase variation locus of *Salmonella enterica* involved in control of O-antigen chain length. PLoS One 7:e36863.

19. Sørensen MCH, van Alphen LB, Harboe A, Li J, Christensen BB, Szymanski CM, Brøndsted L. 2011. Bacteriophage F336 recognizes the capsular phosphoramidate modification of *Campylobacter jejuni* NCTC11168. J Bacteriol 193:6742–6749.

20. Anjum A, Brathwaite KJ, Aidley J, Connerton PL, Cummings NJ, Parkhill J, Connerton I, Bayliss CD. 2016. Phase variation of a Type IIG restriction-modification enzyme alters site-specific methylation patterns and gene expression in *Campylobacter jejuni* strain NCTC11168. Nucleic Acids Res gkw019.

21. Sekulovic O, Ospina Bedoya M, Fivian-Hughes AS, Fairweather NF, Fortier L-C. 2015. The *Clostridium difficile* cell wall protein CwpV confers phase-variable phage resistance. Mol Microbiol 98:329–342.

22. Latino L, Midoux C, Hauck Y, Vergnaud G, Pourcel C. 2016. Pseudolysogeny and sequential mutations build multiresistance to virulent bacteriophages in *Pseudomonas aeruginosa*. Microbiology 162:748–63.

23. High NJ, Jennings MP, Moxon ER. 1996. Tandem repeats of the tetramer 5'-CAAT-3' present in *lic2A* are required for phase variation but not lipopolysaccharide biosynthesis in *Haemophilus influenzae*. Mol Microbiol 20:165–74.

24. Weiser JN, Pan N. 1998. Adaptation of *Haemophilus influenzae* to acquired and innate humoral immunity based on phase variation of lipopolysaccharide. Mol Microbiol 30:767–75.

25. Hosking SL, Craig JE, High NJ. 1999. Phase variation of *lic1A*, *lic2A* and *lic3A* in colonization of the nasopharynx, bloodstream and cerebrospinal fluid by *Haemophilus influenzae* type b. Microbiology 145 (Pt 1:3005–11.

522 26. Poole J, Foster E, Chaloner K, Hunt J, Jennings MP, Bair T, Knudtson K,
523 Christensen E, Munson RS, Winokur PL, Apicella MA. 2013. Analysis of
524 nontypeable *Haemophilus influenzae* phase-variable genes during experimental
525 human nasopharyngeal colonization. J Infect Dis 208:720–7.
526 27. Fox KL, Atack JM, Srikhanta YN, Eckert A, Novotny L a, Bakaletz LO, Jennings
527 MP. 2014. Selection for phase variation of LOS biosynthetic genes frequently
528 occurs in progression of non-typeable *Haemophilus influenzae* infection from the
529 nasopharynx to the middle ear of human patients. PLoS One 9:e90505.
530 28. Brockhurst M, Buckling A, Rainey PB. 2006. Spatial heterogeneity and the
531 stability of host-parasite coexistence. J Evol Biol 19:374–9.
532 29. Palmer M, Lipsitch M, Moxon ER, Bayliss CD. 2013. Broad conditions favor the
533 evolution of phase-variable loci. MBio.
534 30. Dixon K, Bayliss CD, Makepeace K, Moxon ER, Hood DW. 2007. Identification
535 of the functional initiation codons of a phase-variable gene of *Haemophilus*
536 *influenzae*, *lic2A*, with the potential for differential expression. J Bacteriol
537 189:511–21.
538 31. Hedrich AW. 1930. The corrected average attack rate from measles among city
539 children. Am J Epidemiol 11:576–600.
540 32. Brisson M, Bénard É, Drolet M, Bogaards JA, Baussano I, Vänskä S, Jit M, Boily
541 M-C, Smith MA, Berkhof J, Canfell K, Chesson HW, Burger EA, Choi YH, De
542 Blasio BF, De Vlas SJ, Guzzetta G, Hontelez JAC, Horn J, Jepsen MR, Kim JJ,
543 Lazzarato F, Matthijsse SM, Mikolajczyk R, Pavelyev A, Pillsbury M, Shafer LA,
544 Tully SP, Turner HC, Usher C, Walsh C. 2016. Population-level impact, herd

545 immunity, and elimination after human papillomavirus vaccination: a systematic
546 review and meta-analysis of predictions from transmission-dynamic models.
547 Lancet Public Heal 1:e8–e17.
548 33. Sumby P, Smith MCM. 2003. Phase variation in the phage growth limitation
549 system of *Streptomyces coelicolor* A3 (2). J Bacteriol 185:4558–4563.
550 34. Gabig M, Herman-Antosiewicz A, Kwiatkowska M, Los M, Thomas MS,
551 Wegrzyn G. 2002. The cell surface protein Ag43 facilitates phage infection of
552 *Escherichia coli* in the presence of bile salts and carbohydrates. Microbiology
553 148:1533–42.
554 35. Broadbent SE, Davies MR, van der Woude MW. 2010. Phase variation controls
555 expression of *Salmonella* lipopolysaccharide modification genes by a DNA
556 methylation-dependent mechanism. Mol Microbiol 77:337–53.
557 36. Liu M. 2002. Reverse Transcriptase-Mediated Tropism Switching in *Bordetella*
558 Bacteriophage. Science (80-) 295:2091–2094.
559 37. Virji M, Weiser JN, Lindberg AA, Moxon ER. 1990. Antigenic similarities in
560 lipopolysaccharides of *Haemophilus* and *Neisseria* and expression of a
561 digalactoside structure also present on human cells. Microb Pathog 9:441–50.
562 38. Ehrlich R, Miller S, Idoine LS. 1964. Effects of environmental factors on the
563 survival of airborn T-3 coliphage. Appl Microbiol 12:479–82.
564 39. Dubovi EJ, Akers TG. 1970. Airborne stability of tailless bacterial viruses S-13
565 and MS-2. Appl Microbiol 19:624–628.
566 40. Trouwborst T, de Jong JC. 1973. Interaction of some factors in the mechanism of
567 inactivation of bacteriophage MS2 in aerosols. Appl Microbiol 26:252–7.

568 41. Łusiak-Szelachowska M, Zaczek M, Weber-Dąbrowska B, Międzybrodzki R, Kłak
569 M, Fortuna W, Letkiewicz S, Rogóż P, Szufnarowski K, Jończyk-Matysiak E,
570 Owczarek B, Górski A. 2014. Phage neutralization by sera of patients receiving
571 phage therapy. Viral Immunol 27:295–304.
572 42. Christen M, Beusch C, Bösch Y, Cerletti D, Flores-Tinoco CE, Del Medico L,
573 Tschan F, Christen B. 2016. Quantitative Selection Analysis of Bacteriophage
574 φCbK Susceptibility in Caulobacter crescentus. J Mol Biol 428:419–430.
575 43. Mazzocco A, Waddell TE, Lingohr E, Johnson RP. 2009. Enumeration of
576 bacteriophages using the small drop plaque assay system. Methods Mol Biol
577 501:81–85.
578 44. Kropinski AM. 2009. Measurement of the rate of attachment of bacteriophage to
579 cells, p. 151–155. *In* Methods in molecular biology (Clifton, N.J.).
580 45. Cairns BJ, Timms AR, Jansen V a a, Connerton IF, Payne RJH. 2009. Quantitative
581 models of in vitro bacteriophage-host dynamics and their application to phage
582 therapy. PLoS Pathog 5:e1000253.
583 46. Krysiak-Baltyn K, Martin GJO, Stickland AD, Scales PJ, Gras SL. 2016.
584 Computational models of populations of bacteria and lytic phage. Crit Rev
585 Microbiol 42:942–68.

586

587 **FIGURE LEGENDS**

588 FIG 1. Graphic representation of the oscillating prey assay. This diagram illustrates the
589 methodology for experimental simulation of phage HP1c1 transmission through a 50 %
590 ON meta-population structure. Green circles represent a phage-sensitive Rd 30S culture

591 (*lic2A* ON) while pink circles represent a phage-resistant Rd 30R culture (*lic2A* OFF).
592 (A) Phage are added to an exponential phase culture of the bacterial phase variant with an
593 OD_{600} of 0.01 to a final MOI of 0.01 (i.e. ~1 x 10^6 PFU/mL). (B) Incubation of phage
594 with host at 37ºC for 50 minutes to allow for one viral replicative cycle. (C) Filtration of
595 the phage-bacteria mix through a 0.22 µm filter and titration to determine the phage
596 density at the end of the cycle. (D) Transfer of 600 µL of filtered culture-suspension to
597 5.4 mL of fresh culture of the appropriate phase variant (in this example Rd 30R). (E)
598 Incubation of this new culture at 37ºC for 50 minutes beyond which the process is
599 repeated until a total of 20 cycles have been completed.

600

601 FIG. 2. Oscillating prey assay for phage HP1c1 infections of *H. influenzae* strain Rd
602 populations with varying population structures for *lic2A* expression. Each line represents
603 cycling of the phage through a defined series of cultures of two *H. influenzae* strain Rd
604 phase variants, namely Rd30S (S; *lic2A* ON; phage sensitive) and Rd 30R (R; *lic2* OFF;
605 phage resistant). The population structures are indicated in the legend (e.g. S100, all S;
606 S66, S-S-R-S-S-R; S50, S-R-S-R; etc.). The phage HP1c1 concentration was determined
607 at the end of each cycle. Circles represent the phage titre observed from each of five
608 biological replicates, with the line showing the mean of these replicates.

609

610 FIG. 3. Mathematical model of the impact of sub-population phage resistance/sensitivity
611 composition and dilution rate on phage extinction events. This model simulates
612 transmission of phage HP1c1 through meta-populations of *H. influenzae* strain Rd
613 comprising either phage-sensitive (S, *lic2A* ON) or phage-resistant (R, *lic2A* ON)

614 populations for 105 cycles. In these simulations, the order with which phage met either S
615 or R populations was random but dependent on the probability of encountering a resistant
616 population (*R*). Note that the phage population is classified as extinct if the phage titre
617 falls below the extinction threshold (P_0 = 100) with the density being set to 0 for all
618 remaining subsequent cycles. Panels A and B show examples of model outputs, which
619 are quantified as phage densities log(P). These graphs show six iterations of meta-
620 populations comprising either 75% (i.e. R = 0.25; panel A) or 85 % (i.e. R = 0.15; panel
621 B) phage-sensitive populations. Panel (C) shows the mean proportion of phage extinction
622 events occurring in 200 lineages for 200 combinations of probabilities to encounter R
623 (i.e. 1 = 100 % resistant, 0 = 0 % resistant) and rates of phage loss during transmission
624 after each cycle (inverse dilution rate, C; 0.02 = 2 % of phage carried through in each
625 transfer). Colour correlations are shown on the bar to the right of the graph with 1
626 representing no extinction events while 0 is extinction in all lineages.
627
628 FIG. 4. Illustration of phage survival in spatially-structured sub-populations of *lic2A*
629 phase variants of *H. influenzae*. Phage HP1c1 was passaged through a two-dimensional
630 array of phage-resistant (R) and phage-sensitive (S) populations. The proportion of phage
631 sensitive sub-populations (*lic2A* ON) in each fixed area structure were as follows: (A)
632 100 % *lic2A* ON (S100); (B) 66 % *lic2A* ON (S66); (C) 50 % *lic2A* ON (S50); (D) 50 %
633 *lic2A* ON (R50); (E) 33 % *lic2A* ON (R66); and (F) 0 % *lic2A* ON (R100). Each node
634 represents a well in which phage density was measured. The colour of each node
635 indicates the concentration of bacteriophage detected in a specific well. Lines indicate the
636 route taken starting from a central initiator well with line length being proportional to the

637 number of cycles between each node. All central initiator wells were inoculated with 10^6
638 PFU/mL. (G) shows a box-plot of the distribution of phage densities for each tested well
639 of the fixed-area oscillating prey assays. Densities of phage (PFU/mL) obtained from
640 each test well are represented by a dot for the six distributions of *lic2A* phase variants (x-
641 axis). The boxed area indicates the first to third quartile, the line is the median of all
642 points, and whiskers represent 1.5x the interquartile range. Due to the nature of the small-
643 drop plating methodology employed for phage enumeration the minimum detection
644 threshold at any time point is $3.3x10^1$ PFU/mL.
645
646 FIG. 5 Model of the temporal fluctuations in the relative amounts of phage-sensitive and
647 phage-resistant phase variants for a range of PV rates and selection pressures. PV of the
648 *lic2A* gene results in switching between phage-sensitive (S, *lic2A* ON) and phage-
649 resistant (R, *lic2A* OFF) phase variants. The *lic2A* ON state is however known to mediate
650 serum resistance (see text). This model examines how the rate of *lic2A* PV (β, ON-to-
651 OFF switching; α, OFF-to-ON switching; note that switching rates were obtained from
652 Dixon *et al*. [30]) and the degree of selection (m) against the *lic2A* OFF (i.e. R, the
653 phage-resistant state) expression state influences the relative amounts of the R and S
654 states in a population. All panels show changes in the proportion of R. Three different
655 switching rates were examined: $\beta = 1.89x10^{-4}$, $\alpha = 1.13x10^{-4}$ (A); $\beta = 1.89x10^{-5}$, $\alpha =$
656 $1.13x10^{-5}$ (B); $\beta = 1.89x10^{-3}$, $\alpha = 1.13x10^{-3}$ (C).
657
658 FIG 6. Phase variation of phage resistance genes generates 'bacterial herd-immunity' in
659 bacterial meta-populations. Phase variation of a phage-receptor can generate

660 heterogeneous bacterial meta-populations containing a mix of sub-populations that are
661 either susceptible or resistant to phage infection. High proportions of resistant sub-
662 populations can both hinder phage spread and protect susceptible populations from phage
663 attack. In this figure, we show the routes of phage dissemination through four different
664 bacterial meta-populations. Green circles represent phage-sensitive populations while pink
665 circles are phage-resistant populations i.e. *lic2A* ON and OFF populations in our
666 experimental system. Lines with arrowheads show infection events leading to successful
667 phage replication, while lines with barheads represent directions where phage-resistant
668 populations act as a barricade blocking phage spread. Regions free of arrows are those free
669 of phage. Phage spread is shown for: (A) a 100% phage-sensitive (*lic2A* ON) sub-
670 population; (B) 66% phage-sensitive (*lic2A* ON) sub-populations; (C) 66% phage-resistant
671 (*lic2A* OFF) sub-populations; and (D) 100% phage-resistant (*lic2A* OFF) sub-populations.

672

673 **Supplemental material**

674 Fig. S1 Parameter setting experiments for mathematical modelling.

675 Fig. S2 Fit of mathematical model to experimental data.

676 Fig. S3 Distribution of wells receiving a *lic2A* ON or *lic2A* OFF phase variant of *H.*
677 *influenzae* strain Rd for the 50 % ON (panel A) and 66 % ON (panel B) population
678 structures.

679 Fig. S4 Sampling and transfer regimes for testing phage expansion over a fixed area.

680 Text S1. Modelling the dynamics of PV of the *lic2A* gene of *H. influenzae*

681 Fig. S5 Putative ON/OFF state of the *lic2A* gene from 104 *H. influenzae* strains.

Fig. 1 Graphic representation of the oscillating prey assay.

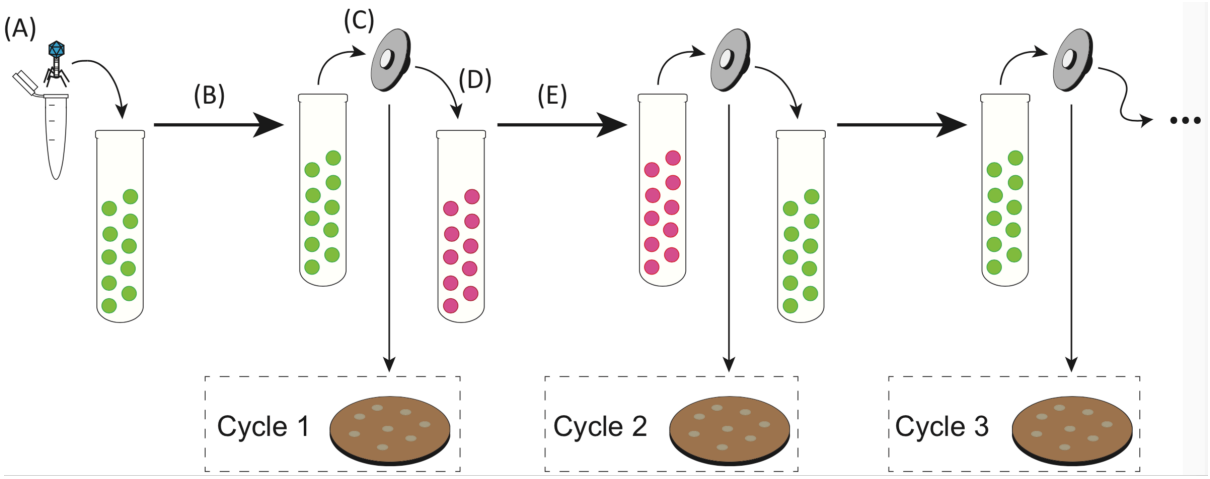

Fig. 2. Oscillating prey assay for phage HP1c1 infections of *H. influenzae* strain Rd populations with varying population structures for *lic2A* expression.

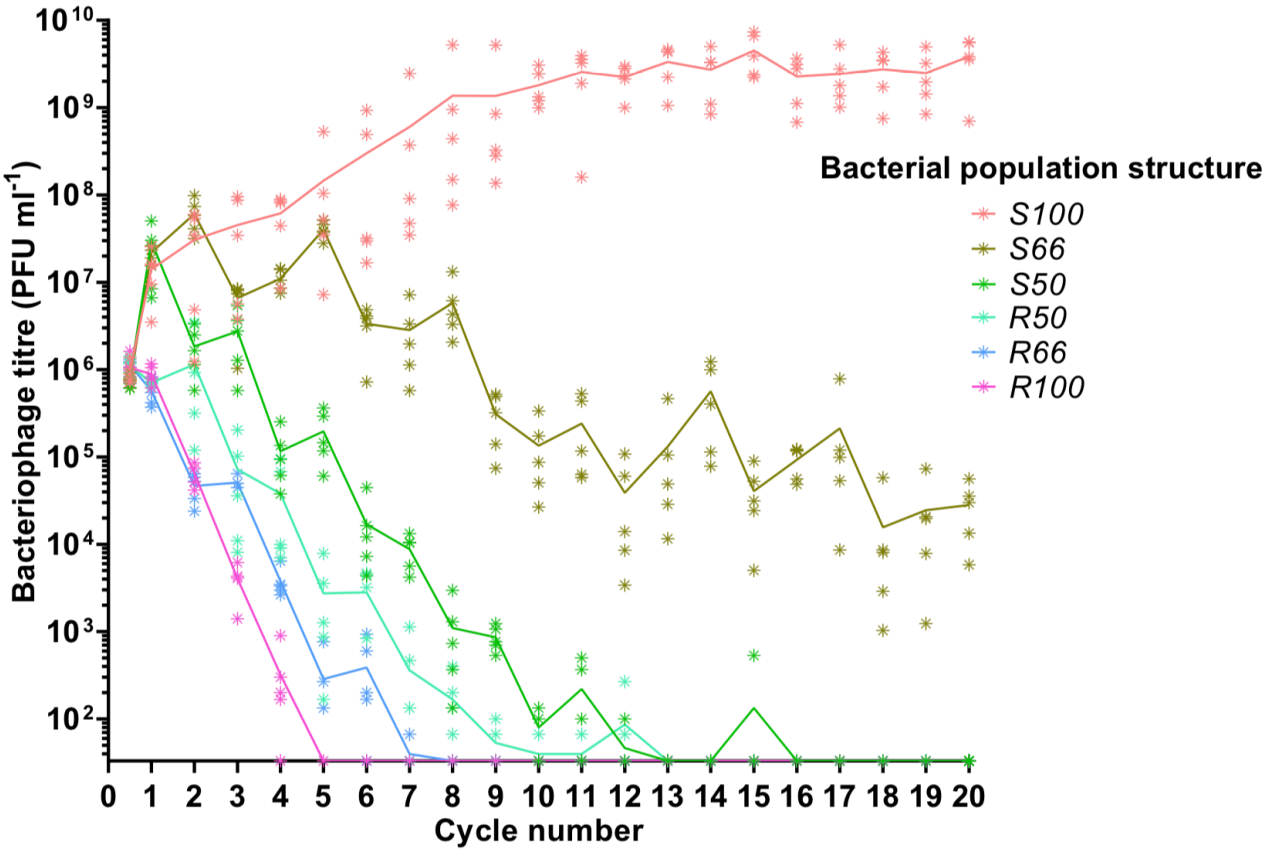

Fig. 3. Mathematical model of the impact of sub-population phage resistance/sensitivity composition and dilution rate on phage extinction events.

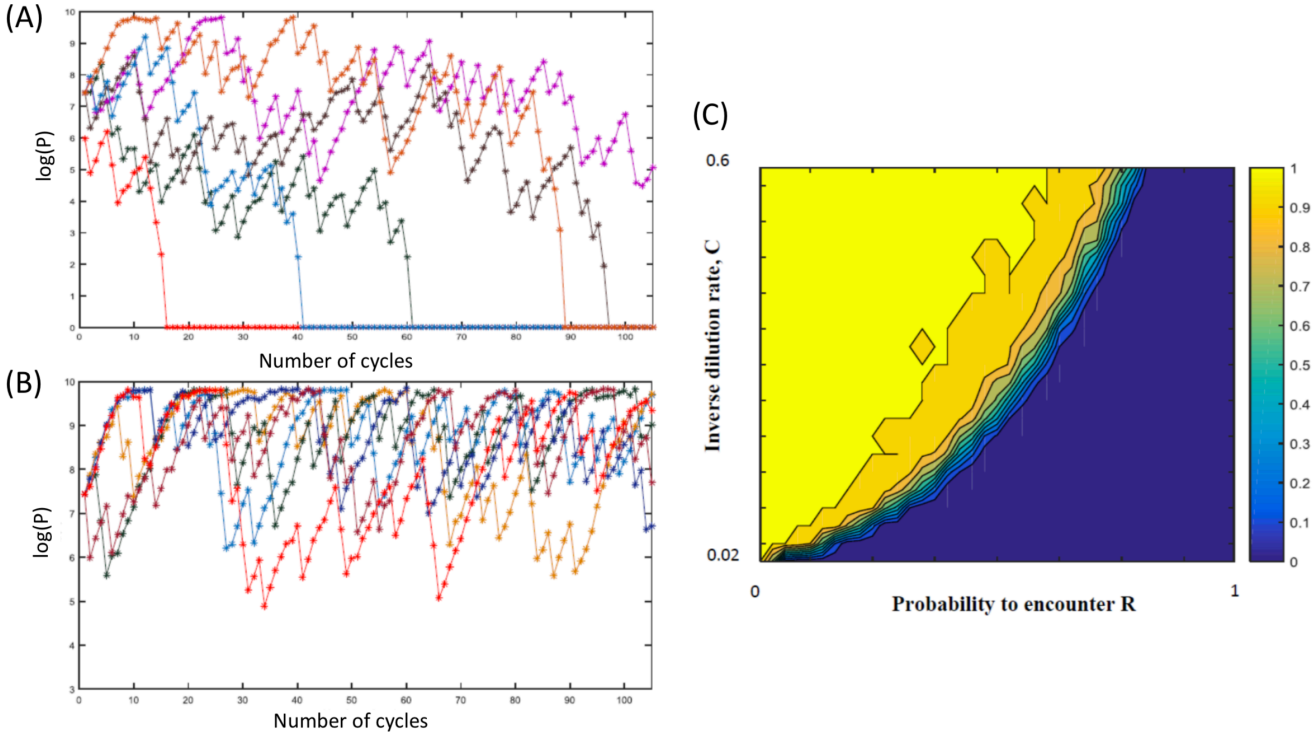

Fig. 4. Illustration of bacteriophage survival in spatially-structured sub-populations of *lic2A* phase variants of *H. influenzae*.

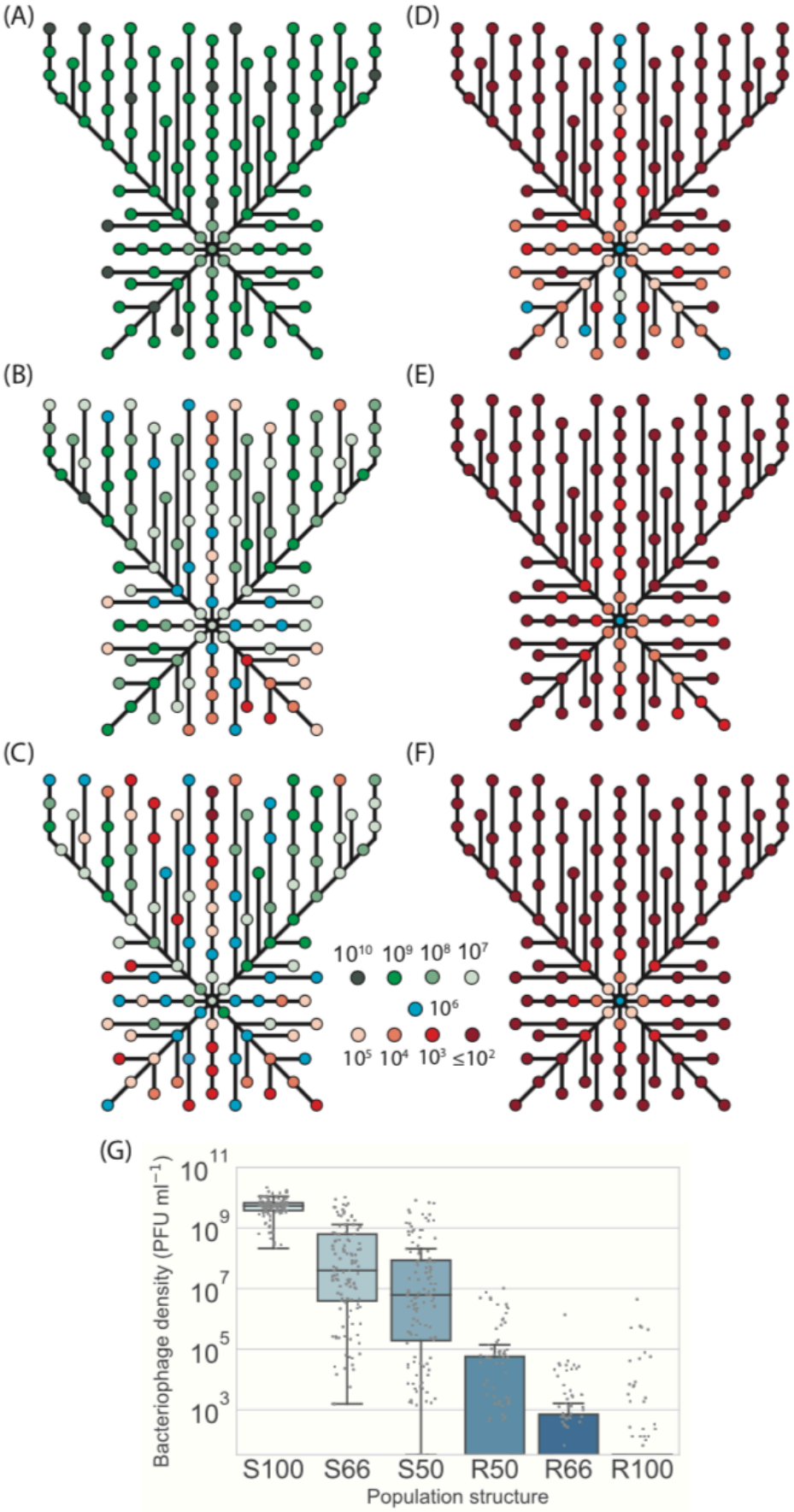

Fig. 5 Model of the temporal fluctuations in the relative amounts of phage-sensitive and phage-resistant phase variants for a range of PV rates and selection pressures.

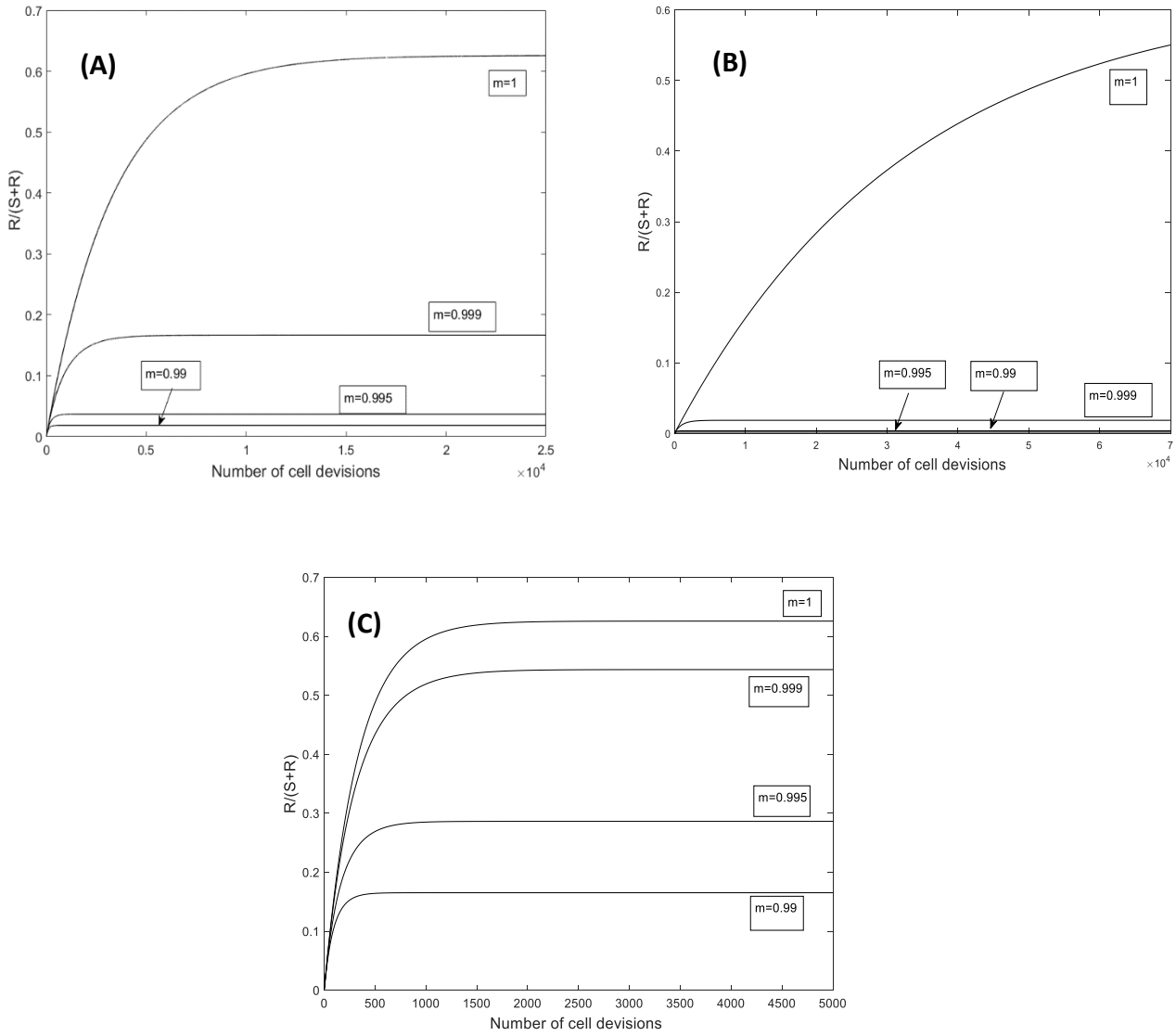

Fig 6. Phase variation of phage resistance genes generates 'bacterial herd-immunity' in bacterial meta-populations